

# USING IN-BED TEMPERATURE PROFILES FOR VISUALIZING THE CONCENTRATION-FRONT MOVEMENT

PAULO CRUZ, ADÉLIO MENDES, FERNÃO D. MAGALHÃES  
University of Porto • 4200-465 Porto, Portugal

Purification of gas streams through adsorption in a packed column is an important process in chemical engineering. The experimental study of such systems involves determination of breakthrough curves for the adsorbable components in the column. Both theoretical and practical implementations of this process are common in undergraduate courses, but students do not readily assimilate some of its aspects. The retention of a concentration front in an adsorbent bed and its implications on the formation of shock waves, for instance, are not easy to visualize mentally, especially when experimental information concerns only the outlet concentration history.

In our senior undergraduate laboratory, we have developed an experiment that has been successful in helping students grasp the concepts of concentration-front movement in fixed beds. Due to the structure of the curricular program, most students actually take this lab course before the advanced separation course in which the theory associated with these processes is detailed. This does not seem to impair the students' ability to interpret and understand the experimental results and theoretical concepts, however.

In addition to the measurement of the outlet breakthrough curve, a set of thermocouples within the bed allows for the indirect "visualization" of the advancement of the concentration front.

A process simulation program, developed for this purpose, also lets students gain sensitivity for the relative importance of the different operation parameters and physical properties. This easy-to-use software is available for downloading at

<http://raff.fe.up.pt/~lepae/simsorb.html>

In this paper we start by briefly describing the Solute Movement Theory, which is a basic tool for interpreting this kind of process, and the mathematical model used in the

software simulation, which involves a more detailed description. Later we will illustrate how students can use both in the interpretation of experimental results.

## THEORETICAL BACKGROUND

A certain gas, A, diluted in an inert carrier gas stream travels in a column packed with a non adsorbent solid at the same velocity as the carrier. If, however, the solid adsorbs gas A, then its velocity will be lower than the carrier's. Simply put, the gas is "retained" by the solid, *i.e.*, it cannot proceed along the column while the adsorption sites are not filled. This idea is more-or-less simple and intuitive.

Things become a bit more complicated, though, when one tries to interpret phenomena such as the formation of different kinds of concentration-front waves. This is when the Solute Movement Theory (SMT) comes in handy. It predicts (for simplified but meaningful conditions) the solute velocity as a function of concentration. Its main result states that an infinitesimal element of solute, with concentration  $c_A$ , will travel the column at a velocity  $u_s$ , which depends (inversely) on the slope of the adsorption isotherm for  $c_A$  ( $dq_A/dc_A$ )

$$u_s = \frac{v}{1 + \rho \frac{1 - \epsilon}{\epsilon} \frac{dq_A}{dc_A}} \quad (1)$$

**Paulo Cruz** is a PhD student in Chemical Engineering at the University of Porto, Portugal. He received his degree in chemical engineering from the same University in 1998. His research interests are in multicomponent mass transport and sorption in porous solids and membranes.

**Adélio Mendes** received his licentiate and PhD from the University of Porto, Portugal, where he is currently Associate Professor. He teaches chemical engineering laboratories and separation processes. His main research interests include membrane and sorption gas separations.

**Fernão Magalhães** is Assistant Professor of Chemical Engineering at the University of Porto, Portugal. He received his PhD from the University of Massachusetts in 1997. His research interests involve mass transport and sorption in porous solids and membranes.

where  $v$  is the interstitial velocity of the inert carrier gas,  $\epsilon$  is the packing porosity,  $\rho$  is the adsorbent's apparent density, and  $q_A$  is the concentration of A adsorbed in the solid, in equilibrium with  $c_A$ . The reader can find the details of our approach for deriving Eq. (1), based on a differential mass balance to the column, at

<http://raff.fe.up.pt/~lepae/simulator.html>

For other approaches see, for example, the book by Wankat.<sup>[1]</sup>

SMT implies, of course, a series of simplifying assumptions, the major being

1. local adsorption equilibrium
2. plug flow in gas phase
3. negligible pressure drop along the column
4. isothermal operation
5. low adsorbate concentration

Assumptions 4 and 5 imply that the interstitial gas velocity can be assumed constant.

It is quite clear, from Eq. (1), that stronger adsorption (higher  $dq_A/dc_A$ ) implies slower solute movement (lower  $u_s$ ). On the other hand, if there is no adsorption, then  $u_s = v$ , and the solute moves at the same speed as the inert carrier gas.

Let us now consider that the column, initially without solute, is subject to an inlet concentration step of magnitude  $c_2$ . Suppose that two well-defined linear regions, as shown in Figure 1, compose the adsorption isotherm for this solute.

Solute elements with concentrations between 0 and  $c_1$  will, according to Eq. (1), have a velocity

$$u_{s1} = \frac{v}{1 + \rho \frac{(1-\epsilon) q_1}{\epsilon c_1}} \quad (2)$$

On the other hand, for solute elements with concentrations between  $c_1$  and  $c_2$  the velocity is

$$u_{s2} = \frac{v}{1 + \rho \frac{(1-\epsilon) (q_2 - q_1)}{\epsilon (c_2 - c_1)}} \quad (3)$$

Velocity  $u_{s1}$  is lower than  $u_{s2}$ . Due to the particular shape of the isotherm, high concentrations tend to move faster than low ones. This would apparently lead to the situation de-

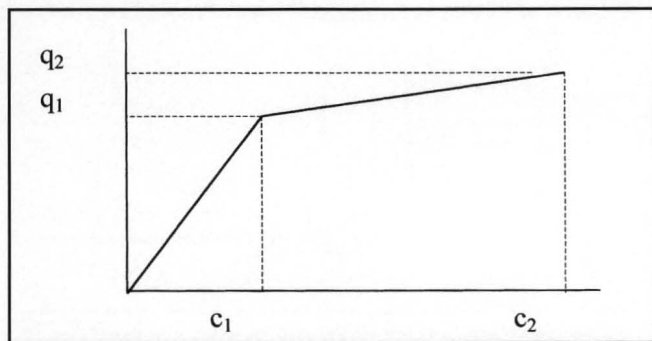


Figure 1. Idealized adsorption isotherm.

picted in Figure 2: high concentrations moving ahead of low concentrations!

This is obviously a physical impossibility. High concentrations cannot exist without the lower ones. What actually occurs is the formation of a shock wave. The concentration front shown on the left in Figure 2 preserves its shape as it moves along the column, with a velocity intermediate between  $u_{s1}$  and  $u_{s2}$ . This velocity can be derived from a mass balance to the shock wave, the result being

$$u_s = \frac{v}{1 + \rho \frac{1-\epsilon}{\epsilon} \frac{q_2}{c_2}} \quad (4)$$

As will be shown later, dispersion effects (not accounted for in SMT) cause the concentration front to develop some distortion as it moves along the column.

And what will happen in the case of desorption, *i.e.*, when, assuming the same isotherm, a negative concentration step is applied at the column entrance (Figure 3)?

Once again, the higher concentrations (between  $c_1$  and  $c_2$ ) tend to move faster. But now these can actually move ahead of the lower ones, causing a progressive deformation of the originally sharp concentration front. We have, then, a dispersive or diffusive wave.<sup>[1]</sup>

This discussion can be easily extended to the analysis of more realistic systems, where the adsorption equilibrium is described by, say, a Langmuir-type isotherm. Such isotherms, where  $dq/dc$  decreases with increasing  $c$ , are called favorable isotherms. It is easy to understand that in the opposite case, *i.e.*, for an unfavorable isotherm, the conditions discussed here for the formation of shock and diffuse waves would be reversed.

The way SMT describes adsorption in a packed column is quite simplistic. More realistic considerations, such as axial

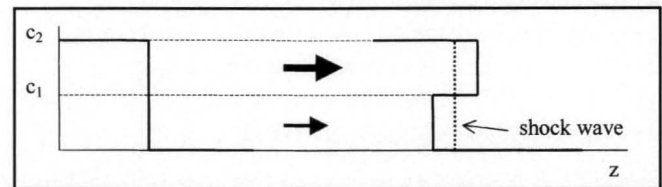


Figure 2. Hypothetical progression of a step in concentration, corresponding to the isotherm shown in Figure 1. This is the basis for the formation of shock waves.

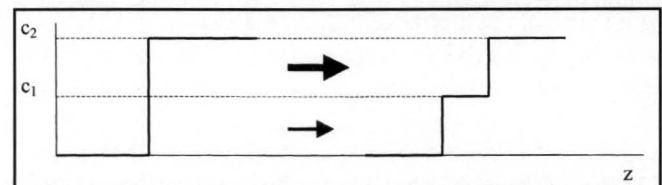


Figure 3. Hypothetical progression of a negative step in concentration, corresponding to the isotherm shown in Figure 1. This would be a dispersive wave.

dispersion, intra-particle mass transport resistance, and non-isothermal behavior, can be added if one establishes a more complex mathematical model for this process. The differential mass and energy balances of our “complex model” (CM) are presented in the Appendix.

Students are expected to be able to interpret each term in the balance equations, even though the resolution of a system of partial differential equations is beyond their abilities. For that we supply our homemade software *simsorb*, which uses finite difference discretization of the spatial coordinate (routine PARSET from package FORSIMVI) and performs the time integration with routine LSODA. It uses a MS-Excel interface for inputting the data and for plotting the results. This software is available for downloading at

<http://raff.fe.up.pt/~lepae/simsorb.html>

The input spreadsheet already contains the set of physical parameters and operating conditions used in simulating our experimental results. The adsorption isotherms (of the type Langmuir-Freundlich) were experimentally measured at our lab and the Peclet number (axial dispersion) estimated from an available correlation.<sup>[2]</sup> Values for the global heat-transfer coefficient and the intra-particle diffusion coefficient were not measured directly. They were obtained by fitting the model to experimental results. This is done previously by the class tutor, so when the students run the simulator for the first time they observe a good agreement between the model’s output and their experimental results. Students can later run the simulator with other input data and analyze its effects on the system’s performance. An example of this is given later in this paper.

## INTERPRETING EXPERIMENTAL RESULTS

The previous theoretical introduction is essentially the first contact that students have with Solute Movement Theory. Even if they seem to understand it relatively well, the sedimentation of concepts demands a more tangible, *i.e.*, experimental, approach. Ideally, it would be possible to directly observe the evolution of a concentration front within a packed column. This is, of course, not the case. Only inlet and outlet concentrations are, in principle, accessible. By measuring the temperature at different points in the column’s axis, however, one can obtain indirect information on the behavior of the concentration front along it.

One may point out that the existence of measurable thermal effects is certainly contrary to the SMT’s original hypothesis of isothermal operation. Nonetheless, as long as these are not excessive, a good compromise

can be obtained between the applicability of SMT and an “on-line visualization” of the progress of the concentration front, as we shall see.

For our lab course we use the adsorbate/adsorbent pair CO<sub>2</sub>/activated carbon. Carbon dioxide was chosen since, in addition to being quite safe to work with and having a low cost, it has a high heat of adsorption in activated carbon. We used activated carbon from Chemviron Carbon in the form of extruded pellets (6.3 mm x 3.6 mm).

Our setup is shown schematically in Figure 4. The column is 250 mm long and 50 mm in internal diameter. Seven evenly spaced holes were drilled in its side to allow for insertion of the thermocouples. The column is placed inside an oven. This has a twofold purpose: to keep the surrounding temperature constant (the oven is set to a temperature slightly above room temperature) and to allow for complete regeneration if necessary. Actually, we noticed that for this system (CO<sub>2</sub>/activated carbon), high-temperature regeneration is not needed; pure helium flow at operation temperature suffices for removing the adsorbed CO<sub>2</sub> (within the sensor’s detection limit). The inlet flow rates of helium (the carrier gas) and carbon dioxide are controlled with two needle valves and monitored with electronic flow meters. The outlet concentration of carbon dioxide is measured with an infrared CO<sub>2</sub> sensor. The inlet feed concentration can be checked before starting a run by directing the feed into the sensor through a column by-pass. A data-acquisition system connected to a computer allows for continuous visualization and, if desired, storage of all data (flow rates, temperature, composition).

Students are asked to perform two breakthrough experiments:

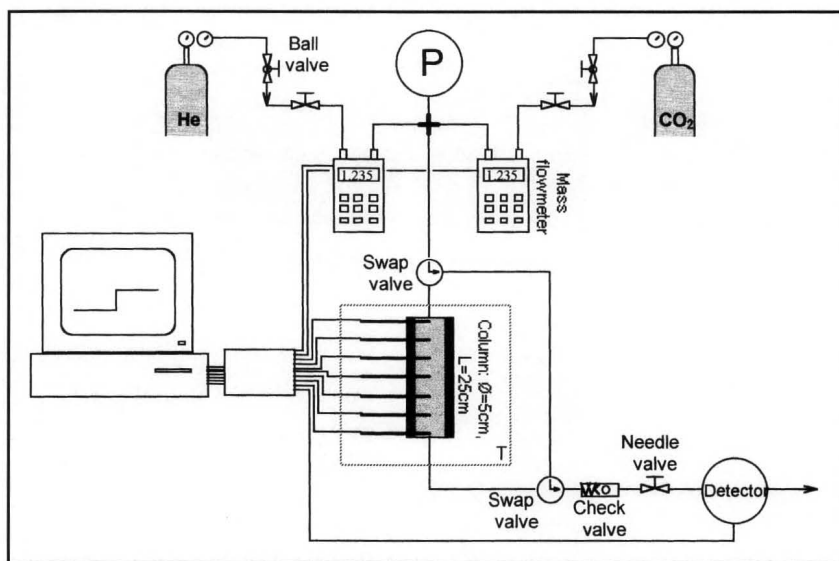


Figure 4. Experimental setup for breakthrough experiments with in-bed temperature measurement.

1. Response to a positive concentration step at the inlet (from pure helium to about 5% mol fraction  $\text{CO}_2$ )
2. Response to a negative concentration step at the inlet (from 5%  $\text{CO}_2$  back to pure helium) after stage 1 has reached steady state.

Complete execution time is about 1.5 hours, leaving enough time for the students to plot the data in the computer and start analyzing the results.

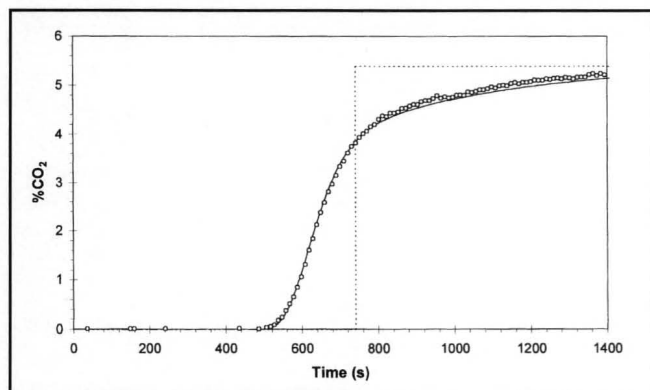
As an example, we next provide some typical plots obtained for the operating conditions listed in Table 1.

The breakthrough curve (*i.e.*, the history of the  $\text{CO}_2$  concentration measured at the column's outlet) obtained for a positive concentration step is shown in Figure 5.

As discussed previously, SMT predicts, for a positive inlet step and a favorable isotherm, the formation of a shock wave (a sharp vertical front). On the other hand, the experimental curve shows a notorious tilt and rounded edges. It is actually noticeable—a pronounced “tailing” as the front approaches the steady-state concentration. This departure from “ideality” is associated with dispersion effects that oppose the compressive nature of the front, such as axial dispersion, intra-particle mass transfer resistance, and non-isothermality. Students are asked to identify and discuss these phenomena. By using the software simulator, they will actually be able to identify the predominant dispersive effect in this case.

**TABLE 1**  
Operating Conditions

Operation Temperature (°C)	Ambient Pressure (Pa)	Operation Pressure (Pa)	Helium Flowrate ( $\text{m}^3(\text{PTN})/\text{s}$ )	Carbon Dioxide Flowrate ( $\text{m}^3(\text{PTN})/\text{s}$ )
38.1	$1.00 \times 10^5$	$2.60 \times 10^5$	$4.35 \times 10^{-5}$	$2.48 \times 10^{-6}$



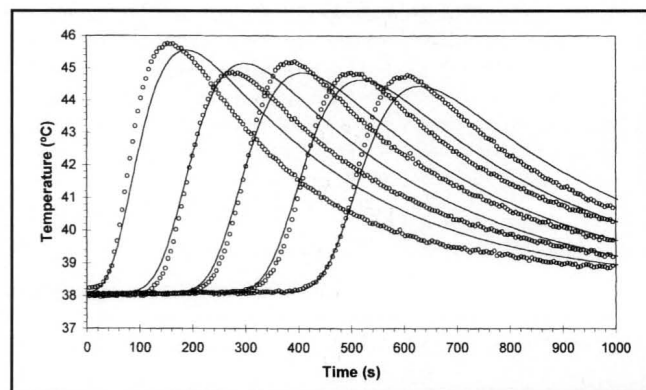
**Figure 5.** Breakthrough curve (exit  $\text{CO}_2$  mol fraction as a function of time) for a positive concentration step at the inlet. The solid line refers to the fit of the complex model. The dashed line is the result from Solute Movement Theory: an ideal shock wave with breakthrough time computed from Eq. (4).

Figure 6 shows the corresponding temperature histories along the column. Data from the last thermocouples are not shown since they are placed at the beginning and at the end of the packed bed where heat is being dissipated through the column's inlet and outlet flanges. This effect masks the temperature information provided by the two thermocouples. Thermocouples 2 and 6, on the other hand, depict quite well the progress of the concentration front along the column.

The observed increase in temperature is associated with the exothermal adsorption of  $\text{CO}_2$  at the concentration front. The significant amplitude of the temperature increase (about  $7^\circ\text{C}$ ), as well as the long length of time that it takes for cooling down, usually surprises the students. It is a good way to make them start questioning the validity of the isothermality hypothesis, often applied without proper reflection in chemical engineering problems.

A more subtle observation is associated with the successive broadening of the temperature peaks along the column or, more clearly visible, the decrease in the temperature maximum measured in each thermocouple. Note: the second peak shown in Figure 6 was recorded with a slightly different thermocouple and therefore it has a different response time. Aside from this deviation from the general trend, one may then conclude that this broadening is associated with the increasing dispersion of the concentration front as it travels along the column. Eventually, the dispersive and compressive effects compensate each other at some point in the column and the shape of the front stabilizes. This is the so-called constant pattern regime.<sup>[1]</sup>

Despite the clear evidences of non-isothermality and dispersive effects, students are asked to use SMT (more exactly, Eq. 4) to predict the time it takes for the shock wave to reach each thermocouple and to compare this with the experimental results, using the maximum temperature in each peak as a reference for the passage of the concentration front. Note that (for such a comparison to be meaningful) we have



**Figure 6.** Temperature histories obtained at evenly spaced points inside the column, for a positive concentration step at the inlet. The solid lines refer to the fit of the complex model.



to assume that the temperature front travels in combination with the concentration front. Under some conditions (mainly for adiabatic systems), the temperature front may lead the concentration front.<sup>[3]</sup> The reasonability of our assumption is reinforced by comparing simulated concentration and temperature profiles. In addition, as can be seen from Table 2, there is a good agreement between the SMT estimations and the experimental results. It is remarkable that the simple SMT model still seems to have some predictive value under these operating conditions.

In relation to the desorption step, the resulting breakthrough curve is shown in Figure 7. SMT predicts that a negative concentration step associated with a favorable isotherm leads to a diffuse wave. The presence of other dispersion phenomenon adds to this effect, causing the experimental concentration front to have a very pronounced tilt.

Figure 8 shows the temperature history profiles. The peaks are now inverted, since desorption is an endothermic process. Now there is a clear broadening of the peaks as the front travels along the column, agreeing with its dispersive nature (in addition to the aforementioned dispersion phenomena).

The qualitative differences between the results obtained from the positive and negative steps are quite evident to the students and contain a lot of material for discussion. The quantitative analysis in terms of SMT is also quite interesting. In addition, students are asked to run the simulation program and to compare its results to the experimental data (see Figures 5 to 8 and Table 2). The complex model, by considering several dispersion effects and non-isothermality, is able to reproduce quite nicely the shapes of the breakthrough curves and temperature peaks.

Students are encouraged to run the simulator with other input parameters and therefore gain sensitivity to how these affect the results. It is particularly interesting to study those

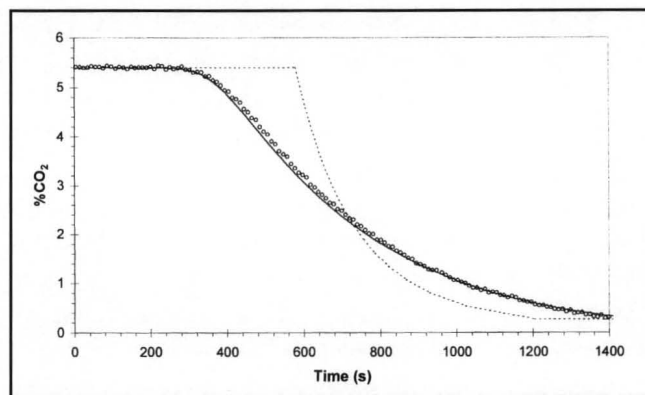


**Figure 7.** Breakthrough curve (exit  $\text{CO}_2$  mol fraction as a function of time) for a negative concentration step at the inlet. The solid line refers to the fit of the complex model; the dashed line is the result from Solute Movement Theory, with breakthrough times for each concentration computed from Eq. (1).

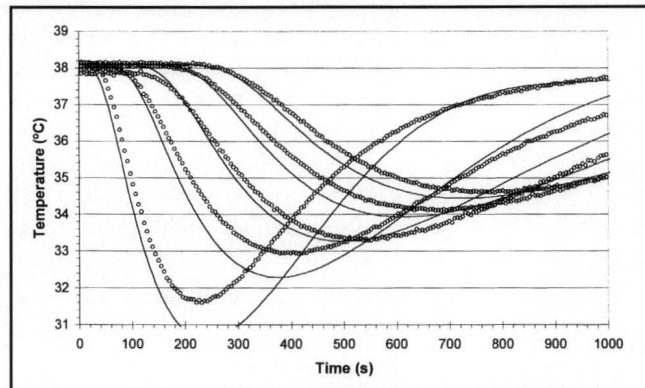


**Figure 8.** Temperature histories obtained at evenly spaced points inside the column for a negative concentration step at the inlet. The solid lines refer to the fit of the complex model.

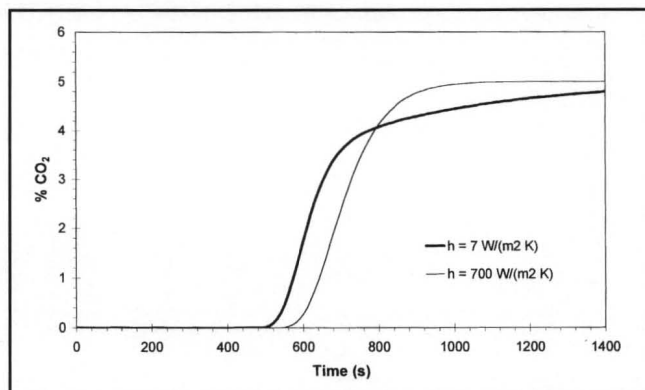


**Figure 9.** Breakthrough curves obtained with the complex model for two different values of the global heat-transfer coefficient,  $h$ . The value  $h=7\text{W}/(\text{m}^2\text{K})$  is the one used in fitting the experimental data (Figures 5 to 8). The value  $h=700\text{W}/(\text{m}^2\text{K})$ , on the other hand, is equivalent to assuming that heat transfer to the exterior is instantaneous.

**TABLE 2**

**Time for the Concentration Front to Reach Each Thermocouple Position**

The experimental time refers to the time when the maximum temperature is reached, the theoretical time from SMT uses Eq. (4), and the theoretical time from CM uses the results from the complex model simulations.

Thermocouple position (m)	Experimental time (min)	Theoretical time from SMT (min)	Theoretical time from Cm (min)
0	-	0.0	0
0.042	3.0	2.1	2.3
0.083	4.8	4.2	4.2
0.125	6.6	6.3	6.2
0.167	8.4	8.4	8.3
0.208	10.3	10.4	10.5
0.250	12.1	12.5	12.5

parameters that are probably more difficult (or impossible) to change experimentally, such as the global external heat transfer coefficient, the heat of sorption, or the intra-particle mass-transfer coefficient. For example, increasing the global heat-transfer coefficient gives rise to a quite different breakthrough curve (see Figure 9). The outlet concentration front is now much closer to a perfect sigmoid, approaching steady state much more rapidly. This seems to indicate that heat accumulation inside the column is the major cause for the "tailing" of the breakthrough curve. As the front passes, the temperature rises significantly, and the amount adsorbed is lower than for isothermal operation. As the column cools down again, the adsorption equilibrium is shifted toward the adsorbed state and more CO<sub>2</sub> is retained in the column. The consequence is that the outlet concentration will take longer to reach steady state.

In addition to complementing the discussion of the results, using the simulation program has an extra pedagogic purpose: it shows students how process modeling in general can be useful in helping to understand and optimize a real system.

## CONCLUDING REMARKS

The experimental study of adsorption in packed beds can be complemented if, in addition to measuring the outlet breakthrough curves, one obtains the temperature histories in different points along the bed. Such an experimental setup is quite simple and economic and provides valuable qualitative and quantitative information that students can process without major difficulties. Solute Movement Theory is a basic tool for that analysis. In addition, using a software simulator based on a more detailed mathematical model provides a better description of the process and allows students to perform "virtual" experiments and understand how different factors

influence the behavior of the adsorption system.

## ACKNOWLEDGMENTS

The authors wish to thank the Chemical Engineering Department for providing financial support for the setup of this experiment.

## NOMENCLATURE

$c_A$	concentration of A in the inter-particle gas phase (mol/m <sup>3</sup> )
$C_{p_g}$	heat capacity of gas (J/mol/K)
$C_{p_s}$	heat capacity of adsorbent (J/kg/K)
$D_{ax}$	axial dispersion coefficient (m <sup>2</sup> /s)
$D_i$	intra-particle diffusion coefficient (m <sup>2</sup> /s)
$h$	overall heat-transfer coefficient (J/m <sup>2</sup> /K/s)
$P$	pressure (Pa)
$q_A$	concentration of A adsorbed in the solid (mol/kg)
$\bar{q}_A$	average concentration of A adsorbed in the solid (mol/kg)
$R_b$	bed radius (m)
$r_p$	particle radius (m)
$t$	time (s)
$T$	temperature (K)
$u_s$	interstitial solute velocity (m/s)
$v$	interstitial carrier gas velocity (m/s)
$z$	axial coordinate (m)

### Greek Letters

$\Delta H$	heat of adsorption (J/mol)
$\epsilon$	packing porosity
$\mathfrak{R}$	gas constant
$\rho$	adsorbent's apparent density

## REFERENCES

1. Wankat, P., *Rate-Controlled Separations*, Elsevier Applied Science, London, pp. 239-251 (1990)
2. Edwards, M.F., and J.F. Richardson, "Gas Dispersion in Packed Beds," *Chem. Eng. Sci.*, **23**, 109 (1968)
3. Yang, R.T., *Gas Separation by Adsorption Processes*, Imperial College Press, London, pp. 161-165 (1997) □

## APPENDIX

The main assumptions of the model are:

1. Plug flow with axial dispersion
2. Negligible radial gradients
3. Negligible pressure drop
4. Variable interstitial velocity
5. Instantaneous thermal equilibrium between stationary and mobile phases
6. Negligible thermal axial dispersion
7. Constant heat capacities
8. Intra-particle mass transport described by linear driving force model
9. Negligible film mass transfer resistance
10. Helium does not absorb
11. No heat accumulation at the wall

Global mass balance (where the total concentration has already been rewritten as a function of total pressure - assumed constant - and

temperature):

$$\frac{\partial v}{\partial z} - \frac{v}{T} \frac{\partial T}{\partial z} + D_{ax} T \frac{\partial}{\partial z} \left( \frac{1}{T^2} \frac{\partial T}{\partial z} \right) - \frac{1}{T} \frac{\partial T}{\partial t} + \frac{\mathfrak{R}T}{P} \frac{1-\epsilon}{\epsilon} \rho \frac{\partial \bar{q}_A}{\partial t} = 0 \quad (A1)$$

Inter-particle solute mass balance

$$\frac{\partial (vc_A)}{\partial z} - D_{ax} \frac{\partial^2 c_A}{\partial z^2} + \frac{\partial c_A}{\partial t} + \frac{1-\epsilon}{\epsilon} \rho \frac{\partial \bar{q}_A}{\partial t} = 0 \quad (A2)$$

Intra-particle solute mass balance (using the linear driving force model)

$$\frac{\partial \bar{q}_A}{\partial t} = \frac{15D_i}{r_p^2} (q_A - \bar{q}_A) \quad (A3)$$

Energy balance

$$\epsilon \frac{P}{\mathfrak{R}T} v C_{p_g} \frac{\partial T}{\partial z} + \left[ \epsilon \frac{P}{\mathfrak{R}T} C_{p_g} + \rho(1-\epsilon)C_{p_s} \right] \frac{\partial T}{\partial t} - \Delta H \rho(1-\epsilon) \frac{\partial \bar{q}_A}{\partial t} + \frac{2h}{R_b} (T - T_a) = 0 \quad (A4)$$